Vol. 36 (2005) *ACTA PHYSICA POLONICA B* No 5

ON THE APPLICATION OF DFA TO THE ANALYSIS OF UNIMODAL MAPS*

Mariusz Sozański† and Jan Żebrowski

Faculty of Physics, Warsaw University of Technology
Koszykowa 75, 00-662 Warsaw, Poland

(Received December 13, 2004)

Dedicated to Professor Andrzej Fuliński on the occasion of his 70th birthday

Chaotic time series obtained from simple dynamical systems (the tent map and the logistic map) are analyzed by means of Detrended Fluctuation Analysis (DFA) — a widely used method for quantifying long-range correlations in time series obtained from complex systems. The first conclusion is that time series obtained from stochastic (noise-driven) and deterministic systems may be indistinguishable using the DFA method. We introduce the adaptive DFA exponent and find that it is related to the structure of the periodic orbit. We show that persistence detected in deterministic series by DFA has a different interpretation than that used in the context of stochastic series analysis. For chaotic time series, we find that only a large level of dynamic additive noise can alter the short-range DFA exponent. Finally, a relation between the DFA exponents and the control parameter of the map is studied. The short-range DFA exponent is sensitive to different kinds of nonlinear transitions — we show that the exponent decreases with the merging of chaotic bands and increases as the natural measure becomes more symmetric. If periodic windows occur in the bifurcation diagram, they can be also detected by DFA as an abrupt decrease of the short-range exponent to a value close to 0. An interior crisis occurs at the end of each periodic window — as a result, the DFA exponent increases as a function of the control parameter until the next band-merging point. As the periodic windows are dense in the bifurcation diagram, the relation of the DFA exponent on the control parameter is more complex for this case.

PACS numbers: 05.45.Tp, 05.40.–a, 02.50.–r

* Presented at the XVII Marian Smoluchowski Symposium on Statistical Physics, Zakopane, Poland, September 4–9, 2004.

† e-mail: `Mariusz.Sozanski@if.pw.edu.pl`

1. Introduction

Natural phenomena occur in a complex and often unpredictable way. Modeling of such phenomena is a challenging task because the variety of behaviors may indicate a variety of unknown underlying processes. If we focus on recent models and measures of natural phenomena [1–27] we find two general approaches.

The first approach originates from statistical physics, where unpredictable events are described by statistical rules. The application of such statistical physics to *e.g.* heart rate variability [1–7], DNA chains [7,14], data from economy [6,15], weather changes analysis [16,17], electric signals [20,21] or stellar X-ray binary systems [22] in principle is equivalent to assuming that these phenomena are caused by truly random processes. This kind of modeling of natural phenomena is also the basis of the Detrended Fluctuation Analysis (DFA) method analyzed in this paper, a recent and already popular method, used extensively in the analysis of various kinds of complex non-stationary data [2–4,14–30].

The second approach is based on the long-known fact that deterministic nonlinear systems may generate seemingly random and unpredictable time series [5,6,8–13]. These series often have the same statistical properties as random processes. Therefore the successful application of stochastic methods of analysis does not exclude the deterministic origin of the data analyzed. Often the source of the processes analyzed is unknown. It may occur that a time series of deterministic origin be assumed of stochastic origin.

The DFA method detects persistency by assuming the self-similarity of series (see, *e.g.*, the study of detecting persistency in fractional Brownian motion by Malamud et Turcotte [31]). The correlations in fluctuations in those signals occur on a statistical basis. We analyze whether the application of DFA to chaotic data is possible — when the "fluctuations" are the result of nonlinearities.

A detailed study on the effect of various transformations of the input signal on DFA can be found in recent papers [28–30]. These transformations include the addition of trends and nonlinearities to the original signal. However, in these studies nonlinearities are treated only as alterations of the signal. Therefore, the main aim of such an analysis consists of eliminating a given set of filters to derive the properties of a presumably "pure" signal. In the cited studies, it is shown that the transform alters the DFA results only at a certain range of correlation lengths. For other correlation lengths, detrended fluctuation analysis of the transformed signal yields the same results as for the unaltered signal. Here we study a different situation — nonlinearity is the genesis of both structure and fluctuations in the analyzed signals [11–13,32], which is in contrast to being just an alteration of the analyzed signal.

In this paper, we investigate the effectiveness of DFA when applied to simple stationary time series derived from two well-known dynamical systems — the logistic map and the tent map. The properties of these systems have been investigated extensively [11–13, 32]. The following equation:

$$x_{n+1} = ax_n(1 - x_n)\,, \tag{1a}$$

defines the logistic map, and the tent map is given by:

$$x_{n+1} = a\left(1 - 2\left|\frac{1}{2} - x_n\right|\right)\,. \tag{1b}$$

In the above equations the control parameter is denoted by a.

Both our own software and that from the authors of the method [33] was used in the calculations.

The paper is divided as follows. First, we introduce the DFA method. In Section 2, we consider the application of DFA to periodic signals. Although from the definition of the method such use of DFA may seem to be inappropriate, we show that, for large periods, the value of the short-range correlations exponent is related to the structure of the periodic orbit. We analyze the sensitivity of the method to noise. The meaning of persistence and antipersistence in the context of deterministic series is discussed. Section 3 is focused on the analysis of the chaotic states of discrete dynamical systems. Finally, in Section 4 we study a general relation between the DFA exponents and the control parameter. We show that DFA is sensitive to different kinds of nonlinear phenomena in deterministic systems. The analogies between the Lyapunov exponent [11–13] and DFA are analyzed. Often it is very difficult to calculate the Lyapunov exponent, as the knowledge of the dynamical evolution of the system is required [6]. Therefore the existence of a possible relation between the Lyapunov exponent and DFA may be an important issue in the analysis of dynamical systems.

1.1. Detrended Fluctuation Analysis

Detrended Fluctuation Analysis is a method for quantifying long-range correlations in non-stationary time series. Among others, it has been applied to detect long-range correlations in DNA nucleotide sequences [14], financial data [15] and mean daily temperatures [16], as well as in coupled chaotic oscillators [20], electric signals [21, 22], stellar X-ray binary systems [23], neural receptors in biological systems [24], cloud structure [25], ethnology [26], music [27] and many other research fields (see [28–30] and references therein for a list of over 70 publications that have utilized DFA). DFA was introduced by Peng *et al.* in 1994 for analyzing nucleotide sequences [14] and soon afterwards applied to heart rate variability (HRV) time series derived from 24-hour ECG recordings [18]. It has been reported to show improved prognostic value for medical diagnosis [3, 5, 19].

As DFA has been originally designed for the DNA walk, one needs to define a general input series-related walk analogously. To do this, the input series $\{B(k)\}$ of length N is integrated after subtracting the average value. The series $\{y(k)\}$ is then:

$$y(k) = \sum_{i=1}^{k} (B(i) - \langle B \rangle) , \tag{2}$$

where $B(i)$ is the i-th point of a discrete time series and $\langle B \rangle$ is the average value of the data. Next, the integrated series is divided into subintervals (windows) of equal length n, and for each window a linear least squares fit to the $y(k)$, denoted $y_n(k)$, is made. The RMS fluctuation around the regression line is then given by the equation:

$$F(n) = \sqrt{\frac{1}{N} \sum_{k=1}^{N} [y(k) - y_n(k)]^2} . \tag{3}$$

The dependence of F on n is examined via a plot of $\log F(n)$ *versus* $\log n$. When scaling occurs, the overall slope of the linear trend in the double-logarithmic scale is equal to the DFA exponent and denoted by $\alpha = \log(e^{-b} F(n))(\log n)^{-1}$, where b is the intercept of the approximated trend. Figure 1 shows an example of the log–log plot of the detrended fluctuations F *versus* window size n for a computer generated uncorrelated random numbers series. The length of the series was 10^5 data points and the DFA exponent is equal to $\alpha = 0.5$.

In Ref. [18], in addition to the global scaling exponent α, α_1 was introduced. This is a short-range correlations exponent, defined for the range of $4 \leq n \leq 16$, as opposed to the whole range of n used in the calculation of α. The importance of the short range correlations for HRV analysis was demonstrated in Refs. [2, 4, 19].

Generally speaking, when a scaling $F(n) \propto n$ is observed, the scaling exponent in the range $0.5 < \alpha < 1$ indicates positive long-range power-law correlations (in other words, *persistence*) and $0 < \alpha < 0.5$ infers anticorrelations (*i.e. antipersistence*) [14, 18, 19]. $\alpha = 1.5$ is obtained for the Brownian walk. The exponent $\alpha = 0.5$ corresponds to uncorrelated data (such as in Fig. 1). If there are short-range correlations, the slope for low n may differ from 0.5 but it will approach this value for large n. It was also proved rigorously that the DFA exponent is related to the Hurst exponent H: $\alpha = 1 + H$

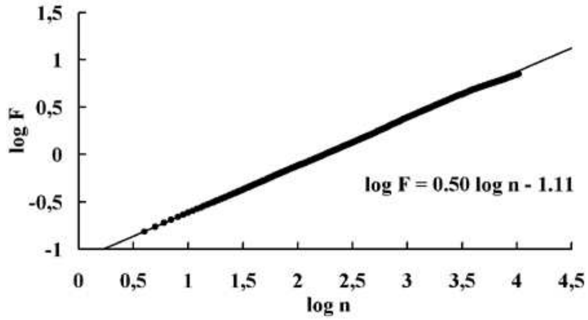

Fig. 1. The dependence of detrended fluctuations F on the window size n for a test series: 10^5 data points calculated using the GNU C compiler random real number generator uniformly distributed from 0 to 1 with a good accuracy; the mean value of the series is 0.500.

when the signal corresponds to an incremental walk (*e.g.* Brownian walk) and $\alpha = H$ when the analyzed signal consists of increments (*e.g.* uncorrelated i.i.d. noise) [34].

Crossovers in the linear dependence of the exponent on window size n have been observed in detrended fluctuation analysis of complex data (*e.g.* biological data) and may be an important indicator characterizing the underlying process [14, 18].

2. Periodic signal analysis

Purely periodic signals have neither a trend nor fluctuations. Therefore the application of DFA to such signal may seem controversial. Although other methods are more suitable for such an analysis, it is interesting to find that, contrary to the assumptions of the definition, it is at all possible to apply DFA to periodic signals. In this section, we introduce two new measures: the DFA short-range adaptive exponent α_+ and the DFA long-range exponent $\underline{\alpha}$. We show that these exponents quantify correlations better than α_1 and α_2 introduced in Ref. [18].

To perform the Detrended Fluctuation Analysis of a periodic state, one must avoid window lengths which are a multiple of the period of the data. Otherwise the fluctuation $F(n)$ vanishes. Figure 2 depicts the DFA plots of periodic states of the logistic map for two values of a. In both cases the period is equal to $p = 18$. In figure 2(a), it can be seen that for most window lengths $F(n)$ is a constant — this makes the resulting overall slope close to 0, which is an indicator of very strong correlations [14, 18] (*i.e.* periodicity in this case). For small values of n, we also observe in Fig. 2(b)

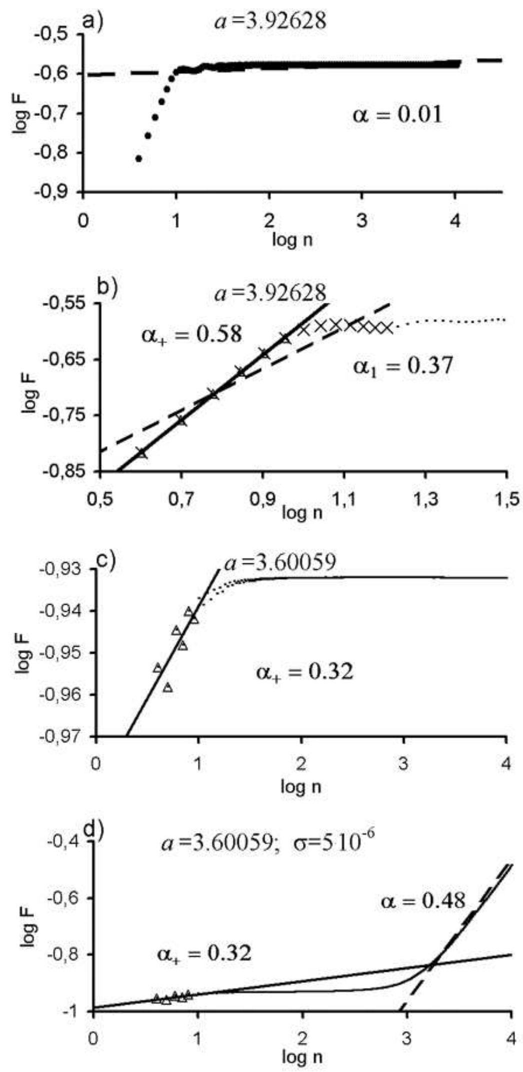

Fig. 2. DFA plots of the logistic map for control parameter a corresponding to periodic states (the period is equal to 18). (a): the overall DFA exponent α is equal to 0 for a periodic state; (b): magnification of the area marked in (a). (c): DFA plot for a periodic orbit with a different structure than in (a). (d): DFA plot for the same parameter value as in (c), but with a small amount of noise ($\sigma = 5 \times 10^{-6}$) added at each iteration. α_1 is the DFA short-range exponent, α_+ is the DFA short-range adaptive exponent and $\underline{\alpha}$ is the DFA long-range exponent.

(a magnification of Fig. 2(a)) the effect of the periodicity of the state analyzed — the fluctuation F depends strongly on the window length. This happens for values of n smaller or of the same order of magnitude as the period length. For such window sizes, the fluctuations F change with n because, at large periods, the series within a window of small size may seem quasiperiodic or almost random. The fluctuation values may then differ strongly from window position to window position along the series. On the other hand, when n is larger than the period length, the series looks alike at all ranges of n larger than the period length and there are very small (if any) differences with window position at a given n.

In summary, for n smaller then the period length, we obtain a slope quite different from zero, while at larger n the DFA exponent tends to zero. This behavior suggests the use of the previously-cited short-range correlations exponent α_1 introduced in [18]. The disadvantage is a rigidly defined range of n required for its calculation ($n \in [4; 16]$). As can be seen in Fig. 2(b), the short-range correlation exponent α_1 (dashed line) differs from zero but its meaning is doubtful due to the large linear approximation error. The error for α_1 will thus be an unknown function of the period of the orbit.

A better approach is to introduce the DFA short-range adaptive exponent α_+ — the slope of the best linear approximation for short-range window sizes n as marked in figure 2(b)–2(d) by a solid line. The points included in the optimized linear regression are denoted by triangles on these plots.

The value of α_1 is equal to 0.37 for the control parameter $a = 3.92628$ in figure 2(b) indicates antipersistence, while the adaptive exponent $\alpha_+ = 0.58$ indicates a weak persistent character of the series (*i.e.* a low level of positive correlations in the series). On the other hand, for the control parameter $a = 3.60059$ the exponent α_+ equal to 0.32 was obtained, indicating antipersistence (Fig. 2(c)). Both series have a period length $p = 18$, the main difference between them is the distribution of the iterations x_i around the mean value $\langle x \rangle$.

The above observations show that the adaptive DFA exponent α_+ is an indicator of the structure of periodic orbits. Such structure can be described by the invariant measure, shown in Fig. 3 for the above discussed periodic orbits. In all plots the structure of the measure depicted is asymmetric. As can be seen for the control parameter $a = 3.92628$ (Fig. 3(a)), although the period of the orbit is 18, there are only ten bars visible, but note that two bars near $x = 0.5$ are twice shorter than the rest. These bars are shorter because they are the effect of a splitting of a single bar. Without this splitting the period would have been 9. The difference in the dynamics of the two orbits in Fig. 3(a) and 3(b) is that, for $a = 3.60059$, the values come one after another in a rather symmetric manner around the mean value (this is equivalent to "antipersistence" in DFA). At $a = 3.92628$, for $x \in [0; 0.4]$

there are only two bars, while in the range [0.6; 1.0] there are six bars. This asymmetric distribution of the elements of the periodic orbit around the mean iterations value makes the series "persistent".

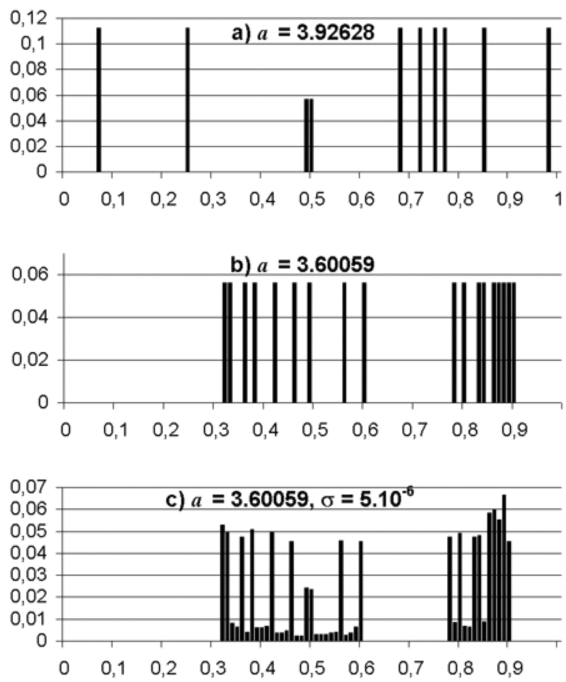

Fig. 3. Invariant measures for the logistic map with control parameter values corresponding to periodic states (compare Fig. 2).

The natural measures depicted in Fig. 4 are a mean representation of the signal in time. DFA is sensitive to the dynamics of the signal. This sensitivity is the consequence of the use in the calculation of the DFA exponents of a sliding window with a varying length n. For example, let the signal structure be asymmetric in the time within one period (as in the case of $a = 3.92628$, see Figs. 2(a) and 3(a)). Then, the fluctuations value F for window sizes n smaller than a half of the period length will be much smaller than those for larger n values (but still not exceeding one period length). As a consequence, the DFA exponent α_+ value will be larger for such a distribution than for a symmetric series of iterations.

By adding even a very small amount of random noise at each iteration of the states in Eqs. (1a) and (1b) (noise amplitude $\sigma = 5 \times 10^{-6}$ at each iteration), we change dramatically the dependence of the mean fluctuation F on n for large window sizes (compare Figs. 2(c) and 2(d)). As in the case of uncorrelated stochastic noise, also in this case, for large n the slope

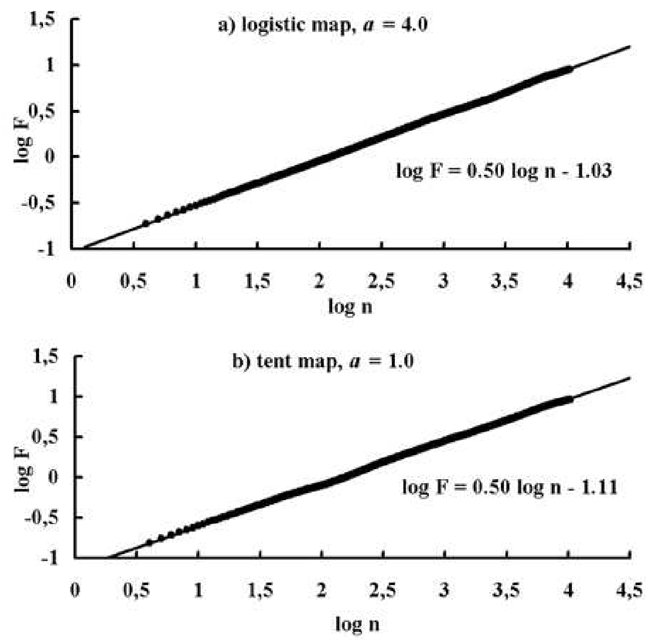

Fig. 4. Double logarithmic plots of the detrended fluctuations F *versus* window size n for two nonlinear unimodal maps. Series length $N = 10^5$. (a) the logistic map with control parameter $a = 4$, (b) the tent map with $a = 1$. The small difference in the intercepts is due to a non-uniform iteration distribution for the logistic map.

will approach the value 0.5 (on Fig. 2(d) this slope is represented by a dashed line). The corresponding DFA exponent calculated for large n will be denoted by $\underline{\alpha}$.

Note that, counter-intuitively, the $\log F$ *versus* $\log n$ plot at small window sizes n remains almost unaltered by the noise. As will be shown in the next section, this is true also for larger levels of additive noise. Note that the value of α_+ did not change due to noise.

The invariant measure for $a = 3.60059$ with noise is shown in Fig. 3(c). With the addition of noise, the fixed points are no longer uniformly distributed and the original natural measure is not preserved. However, the exponent α_+ has the same value as for the series with no noise (Fig. 2(c) and 2(d)). Note that α_+ is a measure of short-range correlations. This indicates that weak dynamic additive noise retains does not destroy short-range correlations. The crossover point (Fig. 2(d)) is a measure of the predictability range of the series [18].

3. Chaotic signal analysis

For fully developed chaos ($a = 4$ for the logistic map and $a = 1$ for the tent map) we cannot distinguish between the time series generated by the maps (1a) and (1b) (Fig. 4) and purely stochastic uncorrelated iid noise (Fig. 1). However, for control parameters even only slightly less than the maximum value at which fully developed chaos is obtained, we find visible traces of determinism at short window lengths (Fig. 5).

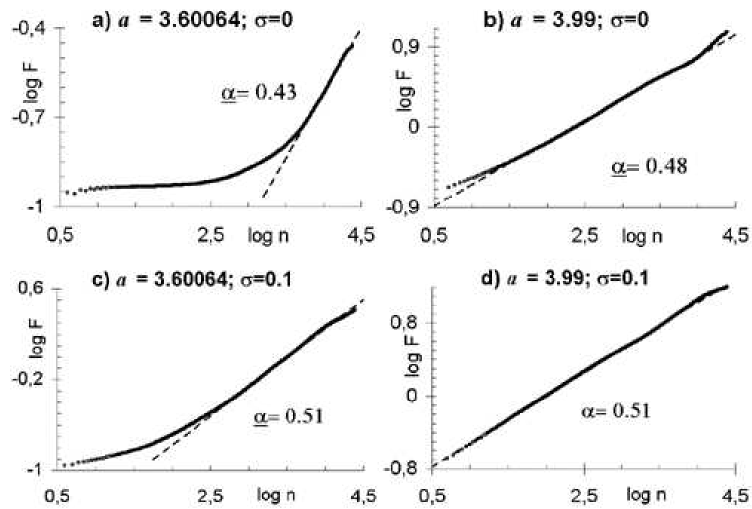

Fig. 5. Double logarithmic plots of the F *versus* n dependence. (a): the logistic map without additive noise for $a = 3.60064$ — a chaotic state. (b): the logistic map without additive noise for $a = 3.99$ — a fully-developed chaotic state. (c): the logistic map with $a = 3.60064$ and large additive noise. (d): the logistic map with $a = 3.99$ and a large additive noise ($\sigma = 0.1$).

The correlation range for the logistic map can be evaluated by means of the DFA scaling exponents. An increase of the DFA exponent value occurs from that obtained for the short n range (*e.g.* $\alpha_1 = 0.03$ for $a = 3.60064$ in Fig. 5(a) and $\alpha_1 = 0.34$ for $a = 3.99$ in Fig. 5(b)) to a value close to 0.5 for large window lengths. This is seen as a crossover on the $\log F(n)$ *versus* $\log n$ plot. Such an effect occurs because, in chaotic states, memory of the initial condition is lost when the number of iterations increases. To illustrate this, we introduce noise which makes the correlation range shorter. This is also a good way to show that the DFA plot does not depend on the genesis of the signal. For example, a periodic series for the logistic map ($a = 3.60059$) with a small amount of additive noise at each iteration (as in Fig. 2(d)) may have a DFA plot similar to the one for a chaotic state series, *e.g.* for

$a = 3.60064$ without noise (Fig. 5(a)). The similarity of the series in this case is expressed by similar values of the short-range correlations exponent α_+, of the long-range correlations exponent $\underline{\alpha}$ and by the sharp change of the slope that occurs approximately at $\log n = 3$.

Other similarities between the DFA plots of different chaotic time series for different control parameter values also can be found. Firstly, we will calculate $\underline{\alpha}$ — the DFA exponent at large window sizes n. For all time series corresponding to chaotic states, the value of this exponent is close to 0.5 indicating the absence of long-range correlations. For a chaotic state series at $a = 3.60064$ without noise (Fig. 5(a)) it is equal to $\underline{\alpha} = 0.43$. For a fully developed chaotic state series the value of $\underline{\alpha}$ is closer to 0.5, *e.g.* $\underline{\alpha} = 0.48$ for $a = 3.99$ (Fig. 5(b)). For time series with a high level of dynamic additive noise ($\sigma = 10\%$) $\underline{\alpha} = 0.51$ (Figs. 5(c) and 5(d)). This shows that the addition of the noise renders the deterministic series for $a < 4$ indistinguishable from each other and from purely stochastic uncorrelated i.i.d. noise by means of DFA at large n. For smaller window sizes (*e.g.* $n < 10^3$) the situation is different.

By adding a relatively high level of dynamic additive noise ($\sigma = 10\%$) to the deterministic time series for $a = 3.60064$ the position of the crossover is shifted to smaller values of n (approximately to $\log n = 2$) and the slope value becomes slightly closer to that for large n (Fig. 5). Thus, the DFA plot in this case (Fig. 5(c)) is more similar to the plots for the series at greater values of the control parameter (as in Fig. 5(b)). This same observation can be obtained for the DFA plot of the time series at $a = 3.99$ (Fig. 5(b)). When dynamic noise is added (Fig. 5(d)) this series becomes indistinguishable by means of DFA from the time series at $a = 4.0$ (Fig. 4(a)) and also from purely stochastic uncorrelated i.i.d. noise (Fig. 1).

Note that for $a < 3.9$ even large noise does not affect strongly the value of α_1 or α_+ (this was also true in the case of periodic signals, compare Figs. 2(c) and 2(d), described in the previous section). More significant is that only a relatively large noise is able to remove completely the correlations detected by DFA. This feature of DFA seems to be important.

The departure from the linear trend at the largest values of n seen in the above described figures is an artifact that occurs because of the small number of sliding windows. At such window sizes (*e.g.* $\log n > 4$ for time series length $N = 10^5$) the number of sliding windows is less than 10. This introduces a large error value in the RMS fluctuation around the regression line from Eq. (3).

4. The dependence of the DFA exponents on the control parameter of the map

Sections 2 and 3 were mostly devoted to the analysis of the DFA plots (*i.e.* $\log F - \log n$ plots) for a particular control parameter value of the logistic map. When the series analyzed were periodic (Section 2), the values of α_1 and α_+ were related to the structure of the periodic orbit and there was no obvious relation between the DFA exponents and the control parameter. In Section 3, it was observed that for larger a corresponding to chaotic states the value of α_1 is also larger and reaches 0.5 for $a = 4$. In this section, we investigate the general relation between the DFA exponent and the control parameter.

The dependence of the properties of chaotic maps on the control parameter is usually described by the Lyapunov exponent [11–13], which is a measure of the memory of the initial conditions. The Lyapunov exponent for one-dimensional iterated maps is calculated as [12]:

$$\lambda = \lim_{N\to\infty} \frac{1}{N} \ln \left| \frac{df(x_i)}{dx_i} \right| , \tag{4}$$

where x_i corresponds to the i-th iteration of the map and x_0 is the initial condition. A negative value of λ indicates periodic states, a positive λ — chaotic states. The Lyapunov exponent is related to the structure of the bifurcation diagram (Figs. 6 and 7). The period doubling points seen on the diagram for the logistic map (Fig. 7) correspond to $\lambda = 0$. The control parameter value at which the doubling cascade becomes infinite is called the accumulation point. For control parameter values greater than the accumulation point, we find chaotic states ($\lambda > 0$) and periodic windows ($\lambda < 0$). In the case of the tent map (Fig. 6), there are no periodic windows (*i.e.* $\lambda > 0$ everywhere beyond the accumulation point), and the dependence of the Lyapunov exponent (denoted by the long dashed line) on the control parameter value a is very simple, namely: $\lambda = \ln(2a)$. The DFA exponent α_1 (lowest curve in Fig. 6) seems to be a more complicated function of the control parameter (we did not calculate α_+ since there are no periodic states in this case).

For a less than 0.6, there is a large scatter in the α_1 values, due to the narrow range in which the iterations fall. Such small variance in effect imitates a periodic signal. For this reason we omitted here the results for this range.

Three different regions may be distinguished for $a > 0.6$. The first region corresponds approximately to $a < 0.7$. In this region, the range of iteration values increases monotonically and so does α_1.

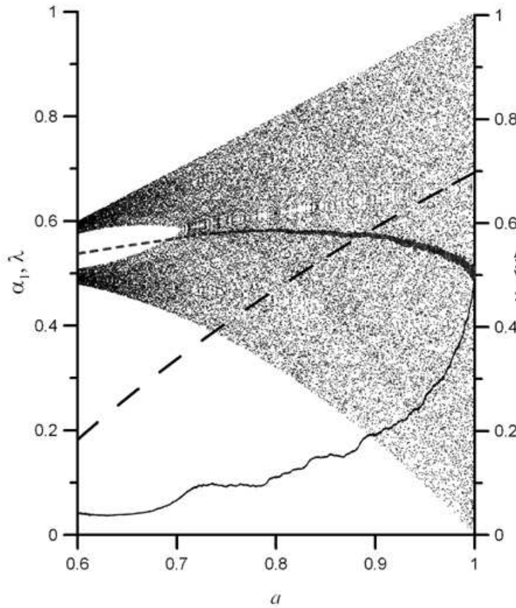

Fig. 6. The Lyapunov λ (long dashed line) and DFA α_1 exponents (continuous line) and mean of the tent map (short dashed line) for $a \in [0.5; 1]$. The bifurcation diagram is drawn in the background for comparison. In the calculation of α_1, α and $\langle x \rangle$ the control parameter was incremented by 10^{-4}, while for the bifurcation diagram by 5×10^{-3}.

The second region (approximately for $0.7 < a < 0.8$) is characterized by a non-monotonic dependence of α_1 on a. The decrease of the DFA exponent value occurs near the point of the band-merging. As the bands merge, the iterations are distributed more uniformly thus the value of α_1 is smaller. But as the control parameter increases, the phase space in the chaotic region also grows (the bifurcation diagram in Fig. 6 widens as we increase a) and so does the DFA exponent. However, because the bifurcation diagram is asymmetric, the increase of this exponent (*i.e.* the decrease of antipersistence) is due to an increase in the symmetry of the natural measure. As a result the DFA exponent is a strong function of the average iteration $\langle x \rangle$. Due to the interplay of the two phenomena: band-merging and increase in the symmetry of the natural measure, many local minima and maxima are observed in this range.

In the third control parameter range ($a > 0.8$), the band-merging has a weak effect, the iterations have a wide range and are mostly uniformly distributed. That is why the DFA exponent grows monotonically in this region.

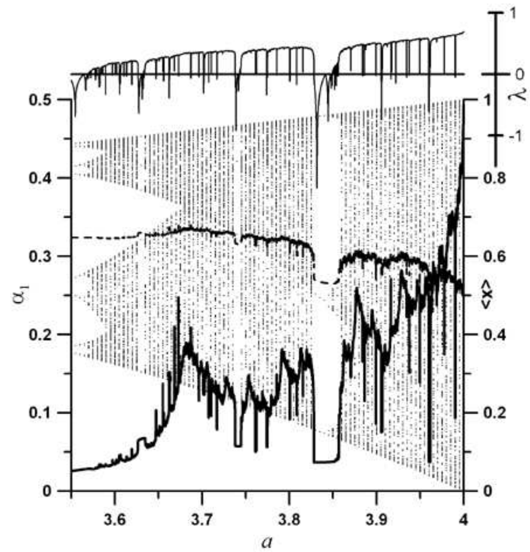

Fig. 7. Upper part: the dependence of λ (Lyapunov exponent, top curve) on the control parameter a for the logistic map. Lower part: the dependence of α_1 (continuous curve) and the mean value calculated for 10000 iterations (dashed curve) on a. In the lower part, the bifurcation diagram is also shown in the background for comparison. In the calculation of α_1, α and $\langle x\rangle$ the control parameter was incremented by 10^{-4}, while for the bifurcation diagram by 5×10^{-3}.

The dependence of α_1 as well as λ on the control parameter and the bifurcation diagram for the logistic map is shown in Fig. 7. Numerous minima of the Lyapunov exponent are seen (indicating periodic windows where $\lambda < 0$) as well as the strong correlation between the abrupt decrease of the Lyapunov exponent below zero and abrupt changes in the value of α_1.

To show that the changes of the two measures are not only correlated but also occur for the same control parameter value, we calculated the value of the critical control parameter values analytically. This can be done by means of symbolic dynamics. To find the value of the control parameter, at which a superstable orbit exists one needs to solve the equation [32]:

$$f(a,x_c) = W(x_c), \tag{5}$$

where x_c is the argument at which the iterated map has the maximum value, $f(a,x_c)$ is the maximum value of the map iterations (equal to $0.25a$ for the logistic map) and W denotes a word composed of symbolic dynamics functions R and L [32]. R denotes the right branch and L the left branch of the map. The symbol C indicating the critical point is in this notation omitted.

The approximate solution of Eq. (5) for the period 3 orbit (in symbolic dynamics denoted RL) is $a = 3.83187$. On the other hand, it can be seen in Fig. 7 that this value of the control parameter corresponds very well to the smallest local minimum of α_1.

The same is true for other superstable orbits, *e.g.* we find local minima of α_1 and λ for period 5 orbits: RL^3 ($a = 3.99027$), RL^2R ($a = 3.90571$) and RLR^2 ($a = 3.73891$). For all of the above control parameter values both the Lyapunov and DFA exponents have a minimum, indicating the presence of a periodic window.

Within periodic windows, α_1 remains almost constant, contrary to λ, which has minima. Thus, in periodic windows we observe almost flat minima or maxima of α_1. Instead, λ for a periodic orbit attains a wide range of values, indicating the strength of attraction of the orbit.

As shown in Section 2, DFA exponents are not good measures for quantifying the periodic behavior of a system — the calculation of α_1 by linear regression is dubious, as in the range $4 < n < 16$ there are often crossovers (see Fig. 2). This was the reason to introduce α_+.

The corresponding relation between α_+ and a value is given in Fig. 8. Note that for the iterated map studied here α_1 never exceeds 0.5, while (as discussed in Section 2) the adaptive DFA exponent α_+ may have values larger than 0.5. In Figs. 7 and 8, both maxima and minima of DFA exponents are observed for the periodic windows. The minima are simple to explain — there are no fluctuations in periodic signals (except for effects due to the

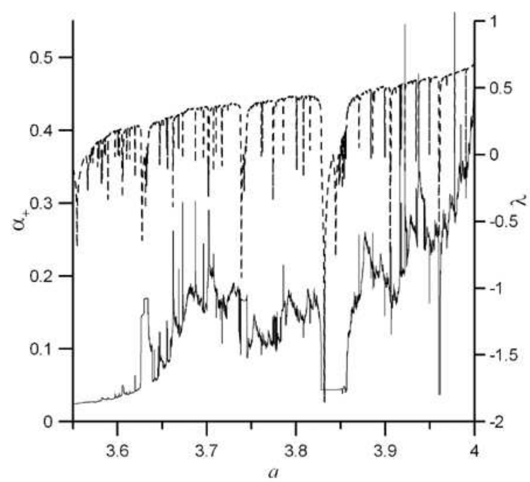

Fig. 8. The dependence of α_+ (the adaptive DFA short-range scaling exponent, continuous line) and λ (Lyapunov exponent, dotted line) on the control parameter a for the logistic map. The control parameter was incremented by 10^{-4}.

sliding window size) therefore the DFA exponent is close to 0 — and constant within the periodic window. On the other hand, the maxima of the DFA exponents occur for periodic time series with an asymmetric distribution of the iteration values within one period (see Section 2).

The complicated dependence of α_1 and α_+ on the control parameter of the logistic map is due to the occurrence of the interior crisis [35]. These are sudden changes in the structure of a chaotic attractor due to collisions with an unstable periodic orbit when the control parameter exceeds a critical value. Similarly as in the case of the tent map, when merging of different chaotic bands occurs, the value of the DFA exponent decreases. In the tent map, this phenomenon practically disappeared when the control parameter exceeded 0.8. For the logistic map, this effect is observed after each of the periodic windows, because of the interior crises within these windows. Beyond the interior crisis point, the DFA exponent increases as a function of the control parameter until the next band-merging point. Then, again,

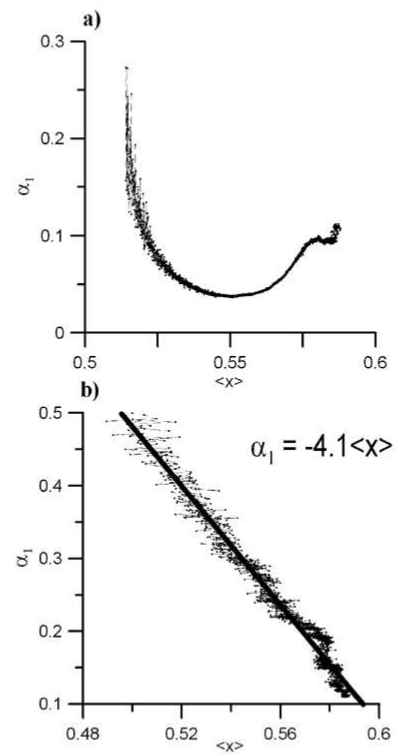

Fig. 9. Relation between the mean iteration value $\langle x \rangle$ and the DFA exponent α_+ for the control parameter ranging from 0.53 to 0.8 (a) and from 0.8 to 1.0 (b) for the tent map. In the latter case, a strong linear dependence is found.

it decreases. However, as the control parameter increases, the phase space in the chaotic region also grows (the widening of the bifurcation diagram in Fig. 7) and so does the DFA exponent. The presence of an infinite number of periodic windows makes the DFA exponent dependence on the control parameter very complex.

In addition to the dependence of the DFA exponent on the control parameter, another relation is worth mentioning. In the case of the tent map, a simple relation between the mean iteration value $\langle x \rangle$ and the DFA exponent α_+ is found. In Fig. 9, we present separate plots representing this relation for $0.53 < a < 0.8$ and for $a > 0.8$. The second plot depicts a strong linear relationship, namely

$$\alpha_+ = -4.1\langle x \rangle + 2.5. \tag{6}$$

The square of the Pearson correlation coefficient for the above relation is equal to 0.97. As mentioned before in the description of Fig. 6, the range of iterations increases monotonically for $a > 0.8$ and so does the DFA exponent α_1. Note that the linear dependence on the mean value is not a general property of DFA exponents, but is due to the properties of the tent map in this region of the control parameter. Due to the asymmetry of the bifurcation diagram, although the phase space grows in this region in both directions, the expansion of the distribution of iterations towards the value of 0 is faster than towards 1. As the iterations are almost monotonically distributed in the phase space for $a > 0.8$, the mean value $\langle x \rangle$ decreases monotonically. In the case of the logistic map, the DFA exponent dependence on the mean value is not as simple.

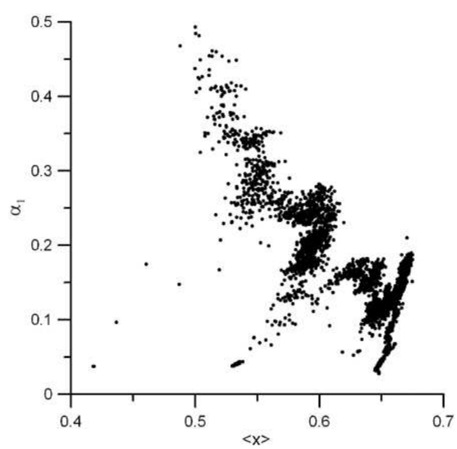

Fig. 10. Relation between the mean iteration value and DFA exponent α_+ for control parameter value ranging from 3.5 up to 4 for the logistic map. The data from within the periodic windows were omitted from this graph.

The dependence seen in Fig. 10 was obtained after omitting the mean iteration values corresponding to periodic windows. The relation is more complex. As there is an infinite set of periodic windows between the accumulation point and the control parameter value corresponding to fully developed chaos, even for the range of control parameter values close to $a = 4$ we do not observe a simple linear dependence of $\langle x \rangle$ on a. The first band-merging point and the occurrence of crises at the end of each periodic window all have an effect on the dependence in Fig. 10. The details of this dependence are being researched.

5. Summary and conclusions

DFA detects and classifies the type of correlations in a time series. We showed that DFA is sensitive to both the dynamics and the statistical properties of the signal. Dynamical systems in a fully developed chaotic state can exhibit random behavior, indistinguishable by means of DFA from stochastic processes. Thus, using the DFA method, it is impossible to state whether the origin of the behavior obtained is a deterministic or noise-driven process. Even if such a method yields consistent results in the analysis of such data as heart rate variability [2,4,14,18,19], it does not mean that the underlying mechanisms are noise-driven processes. An important result obtained by us is that the "persistence" detected in the deterministic series by DFA has a different interpretation than that in a stochastic time series.

We demonstrated that nonlinear maps generate behaviors that can be analyzed by means of DFA. We also applied the DFA method to the analysis of periodic time series. Although, from the definition of the method, this may seem to be inappropriate, we showed that the DFA short-range correlations exponent is related to the structure of the periodic orbits. However, for orbit period length less than 20, the value of the exponent α_1 is often meaningless due to a large linear approximation error. Therefore we introduced the adaptive DFA exponent α_+ as an improved quantifier of the short-range behavior of periodic time series. The new exponent has the lowest possible linear approximation error and reflects the structure of the periodic time series better than α_1.

We studied a general dependence of the DFA short-range exponents on the control parameter a for the tent and logistic maps. In the case of the tent map, the complicated shape of the α_1 *versus* a curve reflects the sensitivity of DFA to the merging of the chaotic bands and the enlarging of the map iterations range with a (Fig. 6).

Periodic windows can be detected by DFA with a good accuracy. The analogies between α_1 and λ shown in this paper (abrupt changes of the DFA exponent at periodic windows, the increase of α_1 with the development of chaos) may suggest that a DFA-related measure could be very useful in such cases where the Lyapunov exponent cannot be easily calculated.

Summarizing, we have shown that DFA may be a useful tool in application to deterministic time series. In some aspects the information obtained is similar to that from the Lyapunov exponent. A general relation between the DFA exponent and the Lyapunov exponent does not exist but the Detrended Fluctuation Analysis may be a useful additional measure in the analysis of chaotic maps and nonlinear systems, as it is sensitive to different types of nonlinear phenomena.

A special feature of DFA exponents α_1 and α_+ is that they are relatively insensitive to noise in the signal. Only relatively large levels of noise can significantly alter the DFA plot of a signal.

This research has been supported by the Warsaw University of Technology internal grant. The authors are very grateful to Peter Talkner for introducing them to the detrended fluctuation method several years ago.

REFERENCES

[1] M. Malik (ed.), *Circulation* **93**, 1043 (1996).

[2] S. Havlin, L.A.N. Amaral, Y. Ashkenazy, A.L. Goldberger, P.Ch. Ivanov, C.-K. Peng, H.E. Stanley, *Physica A* **274**, 99 (1999).

[3] Y. Ashkenazy, M. Lewkowicz, J. Levitan, S. Havlin, K. Saermark, H. Moelgaard, P.E. Bloch Thomsen, M. Moller, U. Hintze, H.V. Huikuri, `physics/9909029`.

[4] T. Mäkikallio, *Analysis of Heart Rate Dynamics by Methods From Nonlinear Mathematics. Clinical Applicability and Prognostic Significance*, Oulun Yliopisto, Oulu 1998.

[5] K. Saermark, M. Moeller, U. Hintze, H. Moelgaard, P.E. Bloch Thomsen, H.V. Huikuri, T. Mäkikallio, J. Levitan, M. Lewkowicz, *Fractals* **8**, 315 (2000).

[6] T. Schreiber, *Phys. Rep.* **308**, 1 (1999).

[7] S.V. Buldyrev, A.L. Goldberger, S. Havlin, C.-K. Peng, H.E. Stanley, Fractals in Biology and Medicine: From DNA to Heartbeat, in: *Fractals in Science*, eds. A. Bunde, S. Havlin, Springer-Verlag, Berlin 1994, pp. 48–87.

[8] B.J. West, *Fractal Physiology and Chaos in Medicine*, World Scientific, Singapore 1990.

[9] J.J. Żebrowski, W. Popławska, R. Baranowski, *Phys. Rev.* **E50**, 4187 (1994).

[10] R.K. Mishra, D. Maaß, E. Zwierlein (eds.), *On Self-Organization. An Interdisciplinary Search for a Unifying Principle*, Springer-Verlag, Berlin 1994.

[11] E. Ott, T. Sauer, J.A. Yorke (eds.), *Coping with Chaos*, Wiley & Sons, New York 1994.

[12] H.G. Schuster, *Deterministic Chaos. An Introduction*, VCH, Weinheim 1988.

[13] C. Robinson, *Dynamical Systems*, CRC Press, 1995.

[14] C.-K. Peng, S.V. Buldyrev, S. Havlin, M. Simons, H.E. Stanley, A.L. Goldberger, *Phys. Rev.* **E49**, 2, 1685 (1994).

[15] N. Vandewalle, M. Ausloos, *Physica A* 246, 454 (1997).

[16] P. Talkner, R.O. Weber, *Phys. Rev.* **E62**, 150 (2000).

[17] E. Koscielny-Bunde, A. Bunde, S. Havlin, H.E. Roman, Y. Goldreich, H.-J. Schellnhuber, *Phys. Rev. Lett.* **81**, 729 (1998).

[18] C.-K. Peng, S. Havlin, H.E. Stanley, A.L. Goldberger, *Chaos* **5**, 82 (1995).

[19] A.L. Goldberger, L.A.N. Amaral, J.M. Hausdorff, P.Ch. Ivanov, C.-K. Peng, H.E. Stanley, *Proc. Natl. Acad. Sci. USA* **99**, suppl. 1, 2466 (2002).

[20] A.N. Pavlov, O.V. Sosnovtseva, E. Mosekilde, *Chaos, Solitons and Fractals* **16**, 801 (2003).

[21] Z. Siwy, M. Ausloos, K. Ivanova, *Phys. Rev.* **E65**, 031907 (2002).

[22] P.A. Varatsos, N.V. Sarlis, E.S. Skordas, *Phys. Rev.* **E68**, 031106 (2003).

[23] M.A. Moret, G.F. Zebende, E. Nogueira, M.G. Pereira, *Phys. Rev.* **E68**, 041104 (2003).

[24] S. Bahar, J.W. Kanthelhardt, A. Neiman, H.H.A. Rego, D.F. Russell, L. Wilkens, A. Bunde, F. Moss, *Europhys. Lett.* **56**, 454 (2001).

[25] K. Ivanova, M. Ausloos, E.E. Clothiaux, T.P. Ackerman, *Europhys. Lett.* **52**, 40 (2000).

[26] C.L. Alados, M.A. Huffman, *Ethnology* **106**, 105 (2000).

[27] H.D. Jennings, P.Ch. Ivanov, A.M. Martins, P.C. da Silva, G.M. Vishwanathan, *Physica A* **336**, 585 (2004).

[28] K. Hu, P.Ch. Ivanov, Z. Chen, P. Carpena, H.E. Stanley, *Phys. Rev.* **E64**, 011114 (2001).

[29] Z. Chen, P.Ch. Ivanov, K. Hu, H. E. Stanley, *Phys. Rev.* **E65**, 041107 (2002).

[30] Z. Chen, K. Hu, P. Carpena, P. Bernaola-Galvan, H.E. Stanley, P.Ch. Ivanov, *Phys. Rev.* **E71**, 011104 (2005).

[31] B.D. Malamud, D.L. Turcotte, *J. Stat. Plan. Infer.* **80**, 173 (1999).

[32] B.-L. Hao, *Elementary Symbolic Dynamics and Chaos in Dissipative Systems*, World Scientific Publishing, Singapore 1989.

[33] The source code of the DFA algorithm written by Peng *et al.* is available at the Physionet Database site (`http://www.physionet.org`). The information about Physionet has been published as: Goldberger AL, Amaral LAN, Glass L, Hausdorff JM, Ivanov PCh, Mark RG, Mietus JE, Moody GB, Peng CK, Stanley HE., Circulation 101, 23, e215 (2000) [Circulation Electronic Pages: `http://circ.ahajournals.org/cgi/content/full/101/23/e215`].

[34] S. Taqqu *et al.*, *Fractals* **3**, 785 (1995).

[35] C. Grebogi, E. Ott, J.A. Yorke, *Phys. Rev. Lett.* **48**, 1507 (1982).